

# Effects of Stirring Speed of Precursor Solution on the Structural, Optical and Morphological Properties of ZnO:Al:Ga Co-Doped Nanoparticles Synthesized via a Facile Sol-Gel Technique

Kiprotich Bett, Sharon Kiprotich\*

Department of Physical and Biological Sciences, Murang'a University of Technology, Murang'a, Kenya

**Abstract** Solar energy offers solutions to the growing demand of energy due to rising population but available silicon-based solar cells are expensive also zinc oxide (ZnO)-based solar cells suffer low efficiency. Therefore the precise control over the material properties is necessary for efficient solar cell technologies, and the properties of ZnO:Al:Ga co-doped nanoparticles are mostly determined by the stirring speed. In this work, we examine the effects of stirring speed on the material properties of ZnO:Al:Ga nanoparticles that have been synthesized for possible use in solar cell technology. Using the sol-gel method technique in conjunction with characterization methods such as FTIR (Fourier-transform infrared spectroscopy), SEM (scanning electron microscopy), XRD (X-ray diffraction) and (UV-Vis) Ultraviolet -visible spectroscopy. This study investigate how the speed of stirring affects the structural, optical, morphological, elemental composition properties of synthesized ZnO:Al: Ga co-doped nanoparticles for possible solar cells. The study revealed that synthesized nanoparticles have enhanced best crystallinity at 1000 rpm, homogeneous doping as shown by SEM micrographs, increased surface area and optimized optical properties that are good for improving solar cell efficiency. This evidence by UV-Vis absorbance at wavelength of 378 nm equivalent to 3.29 eV band gaps which is relatively lower than the standard ZnO's bulk of 3.37 eV. Low energy band-gap of the material is associated with high performance of solar cells. Also XRD reveals stirring speed of 1000 rpm, lattice parameters which are close to standard lattice parameters' of Zinc Oxide. EDX (Energy Dispersive X-ray Spectroscopy) hexagonal wurtzite spectrum confirmed sol-gel technique as simple and inexpensive method of synthesizing nanoparticles as supported by XRD results. In addition, under FTIR, 1000 rpm showed more intense stretching vibrations modes between 400-500cm<sup>-1</sup> that exhibits M-O chemical-bonding in nanoparticles that corresponds to chemical functional composition of Zn-O. These findings pave a way for the logical engineering and design of ZnO:Al:Ga nanoparticles. Furthermore, it explore 1000 rpm as the best stirring speed suitable for synthesizing ZnO:Al:Ga nanoparticles.

**Keywords** ZnO:Al:Ga co-doped nanoparticles, Stirring speed, Sol-gel method, Material properties, Optical properties

## 1. Introduction

The world's growing population demands more sustainable, adequate or sufficient energy for various production of consumer goods for instance industries. Most people uses the traditional sources of energy such as fossils fuels which are not friendly to the environment but adversely affects the climate. Solar energy is potential solution to the arising problem of high demand of energy due to its clean nature and friendly to the environment. With its clean and renewable nature, solar energy has great promise to both reduce environmental pollution and meet the world's energy needs

(Lewis & Nocera, 2006). Zinc oxide (ZnO) solar cells are one of the most popular photovoltaic technologies because of their abundance, sustainability, and unique optoelectronic properties (Liang et al., 2015). Specifically, co-doped ZnO:Al:Ga nanoparticles with gallium (Ga) and aluminum (Al) show improved optical and electrical conductivity, which makes them attractive candidates for efficient solar cell applications (Afre et al., 2010).

Sol-gel synthesis of ZnO:Al:Ga nanoparticles provides a flexible way to modify their material properties to suit solar cell technology needs (OTHMANE et al., 2018). To maximize their performance in photovoltaic systems, control over the material properties such as particle size, crystallinity, and doping must be achieved (Zhou et al., 2018). The stirring speed during the creation of the precursor solution stands out among the other synthesis factors as crucial in determining

\* Corresponding author:

Skiprotich@mut.ac.ke (Sharon Kiprotich)

Received: May 7, 2024; Accepted: May 31, 2024; Published: Jun. 7, 2024

Published online at <http://journal.sapub.org/ajcmp>

the final properties of the prepared nanoparticles (Gatou et al., 2023).

With an emphasis on their applicability to solar cell applications, this study examines the impact of stirring speed on the material properties of ZnO:Al:Ga co-doped nanoparticles produced using the sol-gel method followed by characterization using XRD (X-ray diffraction) and (UV-Vis) Ultraviolet -visible spectroscopy, FTIR (Fourier-transform infrared spectroscopy), SEM (scanning electron microscopy). The study aims to clarify the ideal stirring conditions that facilitate the synthesis of nanoparticles with improved, morphology, structural, elemental, chemical-bonding and optical properties, all of which can further their potential for effective solar energy conversion. In addition, the research helps in growing knowledge on nanoparticle nanotechnology and facilitates the sensible design of ZnO-based materials for use in sustainable solar energy applications which is renewable with no negative effects to the environment or climate. Study and optimization of the growth parameters are key in engineering ZnO:Al:Ga nanoparticles to possess the desired material properties. Effects of pH, growth temperature, reaction time and Ga:Al mole doping concentrations have been reported in the literature (Ungula et al. 2024 and Gakuru et al. 2024). However, research on the effects of stirring speed of the precursor solution on the structural, morphological and optical properties of the ZnO:Al:Ga NPs is scanty. Therefore, this research explores to add to the body of knowledge on the effects of this parameter.

## 2. Methodology

### Materials

Zinc acetate, aluminum nitrate, gallium nitrate, sodium hydroxide pellets, Ethanol, deionized water. All the chemicals used were of analytical grade and used as purchased without any alteration.

### Procedure

To examine the effects of stirring speed of precursor solution on the material properties of ZnO:Al:Ga co-doped nanoparticles for solar cell applications, ZnO:Al:Ga co-doped nanoparticles were prepared from Zinc acetate dehydrate, Aluminum nitrate, gallium nitrate, sodium hydroxide, ethanol and deionized water. In the beaker 2.1951 g of zinc acetate is dissolved with 50 mL of ethanol until formation of clear solution, add drop wise 25 mL of 1M sodium hydroxide, once mixture of zinc acetate, ethanol and sodium hydroxide is formed under constant growth temperature of 75°C, pH value 9 and varying stirring speed of values: 1, 1.5, 2, 2.5, 3, 3.5 and 4 x 10<sup>3</sup> r.p.m. Thereafter, a solution containing 0.187565 g of aluminum nitrate, 0.12787g of gallium nitrate added to the precursor solution and left until duration of one hour is over. The suspension formed of ZnO:Al:Ga was removed from hot plate and allowed to age. The ZnO:Al:Ga nanoparticles then washed with deionized water through decantation. The washed sample was dried for 60 minutes at

120°C in the oven and annealed at 600°C for 1 hour. The ZnO:Al:Ga co-doped nanoparticles samples were taken for characterization using X-ray diffraction (XRD) patterns in the 2θ range, using Cu/Kα radiation ( $\lambda = 1.54056 \text{ \AA}$ ) from an X-ray diffractometer (Model ARL EQUINOX 100 X-Ray Diffractometer), Scanning electron microscopy (SEM) micrographs and Energy Dispersive X-ray Spectroscopy (EDS) Model Phenom XLG2, UV- Spectrophotometer Model UV-1800 SHIMADZU and Fourier transform infrared (FTIR) transmission spectra FTIR Spectrophotometer Model IRspirit SHIMADZU.

## 3. Results and Analysis

### XRD Analysis

ZnO:Al:Ga co-doped nanoparticles have favorable electrical and optical properties that make them promising for use in solar cell applications (Chakraborti et al., 2008). To maximize their performance, it is imperative to understand how synthesis factors like stirring speed affect their material properties. Figure 1(i) shows all synthesized samples, XRD examination showed distinctive peaks compatible with the hexagonal wurtzite structure of ZnO nanoparticles which correspond to the earlier research (Ungula et al., 2017) that matches well with JCPDS No. 79-0208. This consistency attests to the synthesis's success at various stirring rates using sol-gel method.

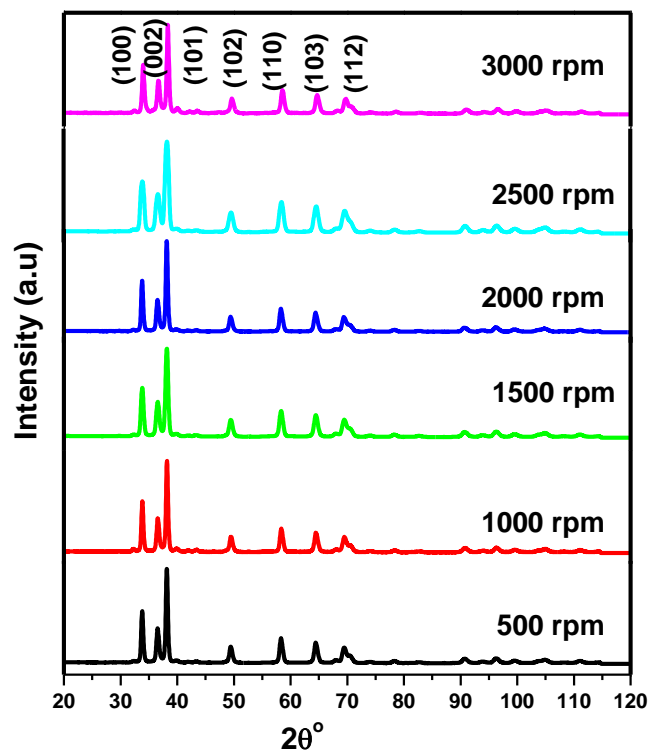


**Figure 1(i).** XRD pattern between 20° – 120° for all synthesized samples of ZnO:Al:Ga co-doped nanoparticles under varying stirring speed

The XRD graph of samples 500 rpm, 1000 rpm, 1500 rpm, 2000 rpm, 2500 rpm, and 3000 rpm shows clear, identical

peak patterns in Figure 1(i), demonstrating the synthesis process' effective in producing nanoparticles. Research indicates that stirring speed has a major impact on crystalline structure, and that stirring circumstances have a considerable impact on the synthesis of nanoparticles (Shaba et al., 2021). The results support these observations by pointing out variations in crystallite size.

The examined peak  $2\theta$  range from  $37.5^\circ$  to  $39.0^\circ$  found significant variations in peak intensity figure 1(ii). The peak

intensity consistently decreases as the stirring speed increases from 500 to 3000 rpm. However, 3000 rpm peak intensity varied from the predicted trend pattern and this indicate the presence of other factors influencing crystallization. These changes were explained by Nagorski (2021) as peak intensity influence the crystallinity and particle size, which is consistent with study's findings of how stirring speed affects peak intensity of nanoparticles by showing different XRD spectrum pattern.

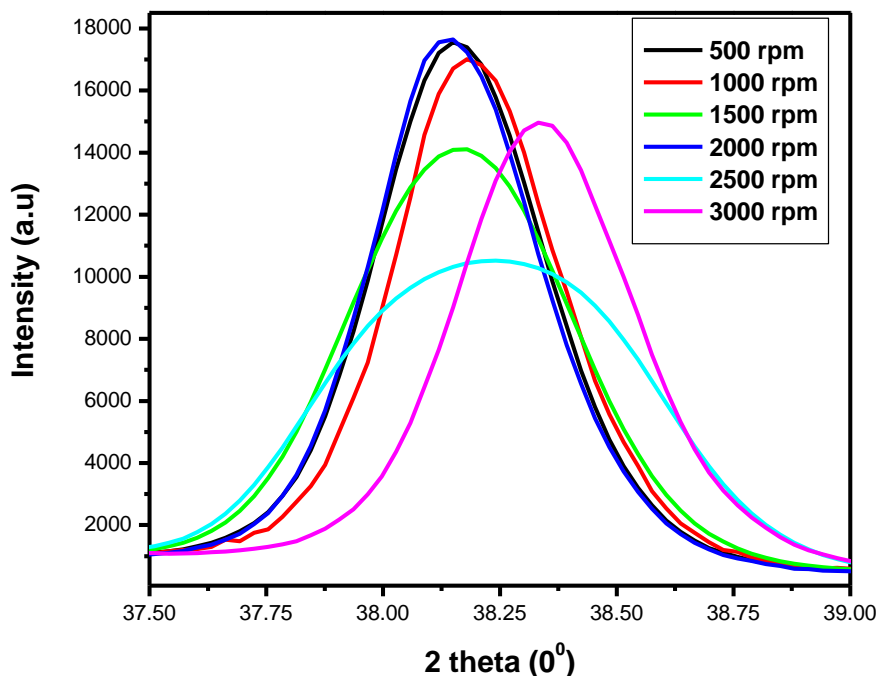


Figure 1(ii). Magnified XRD pattern between  $37.5^\circ$  –  $39.0^\circ$  for the synthesized ZnO:Al:Ga co-doped nanoparticles under varying stirring speed

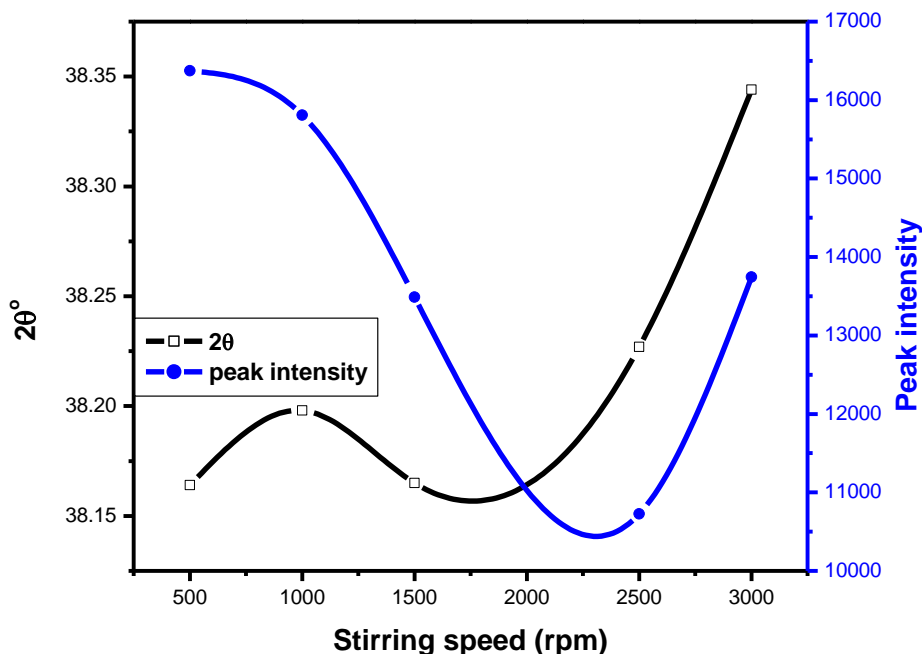


Figure 1(iii). A graph of most intense peak for the synthesized ZnO:Al:Ga co-doped nanoparticles under varying stirring speed

Figure 1(iii) shows the relationship between the  $2\theta$  and peak intensity for the most intense peak that lies between  $37.5^\circ - 39.0^\circ$  for the synthesized ZnO:Al:Ga co-doped nanoparticles under varying stirring speed. The angle  $2\theta$  for the prepared nanoparticles increase with the stirring speed of materials resulting to decrease in the peak intensity of ZnO:Al:Ga nanoparticles as similar results obtained by Kelchtermans (2014). However, the peak intensity showed the decrease with increase in stirring speed up to 2500 rpm then rise. This confirms also reduction in crystallite size as well as quality of nanoparticles.

The lattice parameters were calculated using the equations  $a = \frac{\lambda}{\sqrt{3} \sin\theta}$  and  $c = a \sqrt{\frac{8}{3}}$  where 'a' and 'c' are the lattice parameters. The prepared ZnO:Al:Ga nanoparticles showed 'a' range between 0.2708 – 0.2721 nm and 'c' to be 0.4443 – 0.4422 nm as shown in table 1.

**Table 1.** Showing lattice parameters of prepared ZnO:Al:Ga co-doped nanoparticles

Stirring speed (rpm)	$2\theta$	'a'	'c'
500	38.164	0.2721	0.4443
1000	38.198	0.2718	0.4438
1500	38.165	0.2721	0.4443
2000	38.155	0.2716	0.4435
2500	38.227	0.2716	0.4435
3000	38.344	0.2708	0.4422

The crystallite size was estimated using the Scherrer

equation;  $D = \frac{K\lambda}{\beta \cos \theta}$  (Gherbiet al., 2022) where D is crystalline size, K is constant (0.89),  $\lambda$  is 0.154056 nm, mean wavelength of CuK $\alpha$ 1 radiation,  $\beta$  is full width half maxima and  $\theta$  is Bragg's angle in radians, the average crystallite size analysis, as presented in Table 2 were as follows 21.46, 22.01, 17.19, 21.73, 12.52 and 20.61 nm for 500 rpm, 1000 rpm, 1500 rpm, 2000 rpm, 2500 rpm and 3000 rpm respectively. The obtained lattice parameters and crystallite size of synthesized ZnO:Al:Ga nanoparticles showed minimal changes in the bulk's ZnO standard lattice parameters similar to the research done by Geetha (2020). This affirms the purity of synthesized nanoparticles.

The figure 1(iv) depicted trigonometric curve of FWHM and crystallite size of synthesized ZnO:Al:Ga co-doped nanoparticles for various stirring speeds. The FWHM of the prepared nanoparticles showed increase with the increase of stirring speed in the precursor also reported by Eswar et al., (2020). There was decrease in the crystallite size as stirring speed on the material properties increase with exception of 3000 rpm. This confirmed nanoparticles have undergone strain or existence of imperfections defects in the synthesis of ZnO:Al:Ga nanoparticles.

Therefore, the formula  $\delta = \frac{1}{D^2}$  (Ungula et al., 2024) where  $\delta$  is the length of dislocation density and D is the crystalline size; was applied in order to calculate the dislocation density, as table 3 illustrates the results. Also, table 3 shows the micro-strain ( $\epsilon$ ) values, which were computed using the equation,  $\epsilon = \frac{\beta}{4 \tan\theta}$  (Kiprotich et al., 2022) where  $\theta$  is the diffraction angle and  $\beta$  is the full width at half maximum.

**Table 2.** Showing crystallite size of prepared ZnO:Al:Ga co-doped nanoparticles

	Stirring speed (rpm)	500	1000	1500	2000	2500	3000
$2\theta$	(001)	33.826	33.852	33.829	33.813	33.887	33.999
	(002)	36.565	36.594	36.573	36.552	36.642	36.703
	(101)	38.164	38.198	38.165	38.155	38.227	38.344
$\beta$	(100)	0.36831	0.35666	0.46417	0.36107	0.63155	0.39622
	(002)	0.44483	0.43736	0.53003	0.44477	0.71578	0.44442
	(101)	0.36483	0.35608	0.46973	0.35934	0.66085	0.38177
Peak intensity	(100)	9042.6	8776.6	7460.0	9280.2	5902.9	7430.5
	(002)	5704.0	5538.1	4975.3	5469.1	4122.0	4721.9
	(101)	16373	15808	13490	16426	10725	13743
Crystallite size (D)	(100)	22.54	23.28	17.89	22.99	13.15	20.96
	(002)	18.81	19.13	15.78	18.81	11.69	18.83
	(101)	23.04	23.61	17.89	23.39	12.72	22.03
$D_{average}$		21.46	22.01	17.19	21.73	12.52	20.61

**Table 3.** Showing dislocation density and strain of prepared ZnO:Al:Ga co-doped nanoparticles

Stirring speed (rpm)	500	1000	1500	2000	2500	3000
$\delta$	0.0466	0.0454	0.0582	0.0460	0.0798	0.0485
$\epsilon$	0.2637	0.2571	0.3395	0.2598	0.4767	0.2745

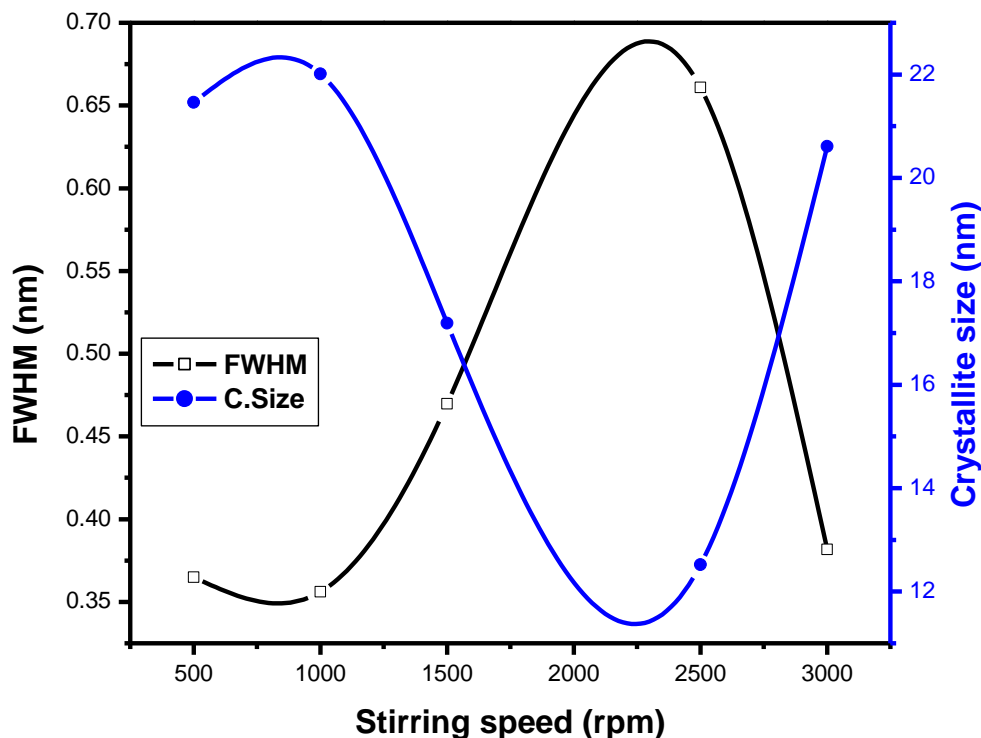


Figure 1(iv). The graph of FWHM and crystallite size of synthesized ZnO:Al:Ga co-doped nanoparticles for various stirring speeds

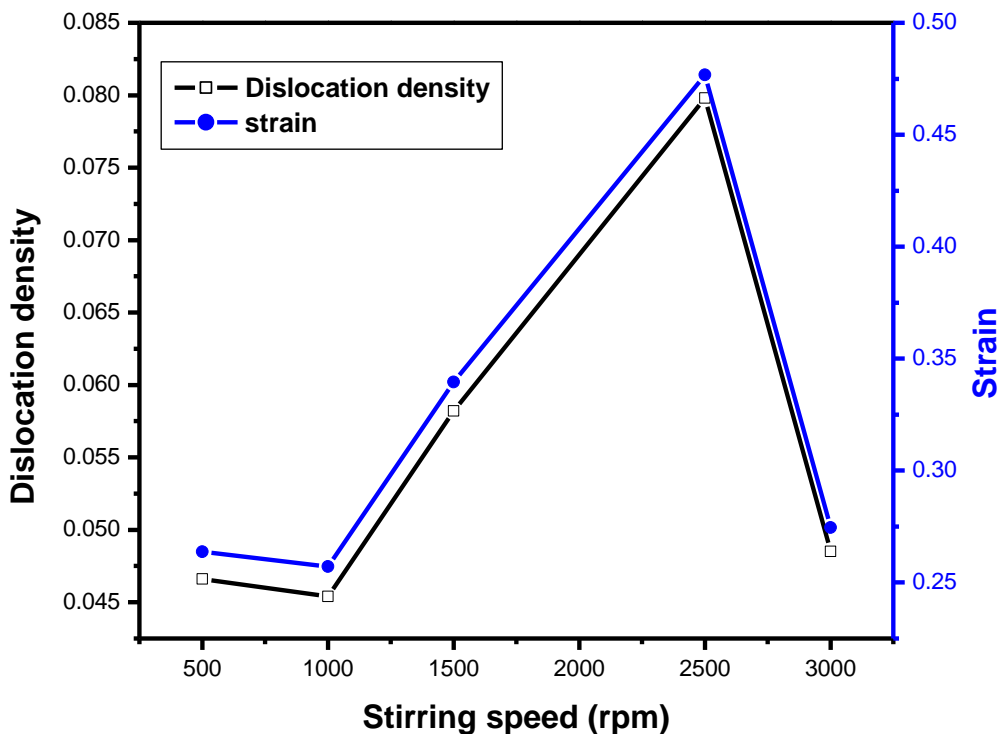


Figure 1(v). The graph of dislocation density and strain of prepared ZnO:Al:Ga co-doped nanoparticles for various stirring speeds

The dislocation density is the concentration or density of dislocations within nanoparticles. Figure 1(v) shows dislocation density and strain impact on the nano-crystal structure of ZnO:Al:Ga nanoparticles where the regular arrangement of atoms is disrupted. The changes in lattice parameters and crystallite size of nanoparticles was due to thermal strain and presence of impurities this corresponds to what Zak

et al., (2024) reported. The figure 1(v) showed increase in the strain and dislocation densities as stirring speeds increase. This affirms the higher dislocation densities and strain the stronger nanoparticles but less ductile nanomaterials, while lower dislocation densities and strain the weaker nanoparticle but more ductile materials. In addition, it also quantifies the change in shape or size of a material relative to its original

dimensions as shown in the difference in lattice parameters with standard of ZnO's bulk values.

### UV- Vis Analysis

ZnO:Al:Ga co-doped nanoparticle characterization demonstrates the value of UV-Vis spectroscopy as a vital tool for understanding the optical properties of materials. The study's prepared nanoparticles' transmittance spectra, shown in Figure 2(i), show clear variations in transmittance

peaks that correlate to different stirring rates throughout the synthesis in the precursor solution. The transmittance spectrum shows the largest peak at 500 rpm, with subsequent peaks at 1500 rpm, 2500 rpm, and 3000 rpm, in that order. This pattern is consistent with earlier research by Khan et al. (2016) and Mukwakwa (2017), who also observed similar changes in transmittance spectra in response to varying synthesis stirring velocities.

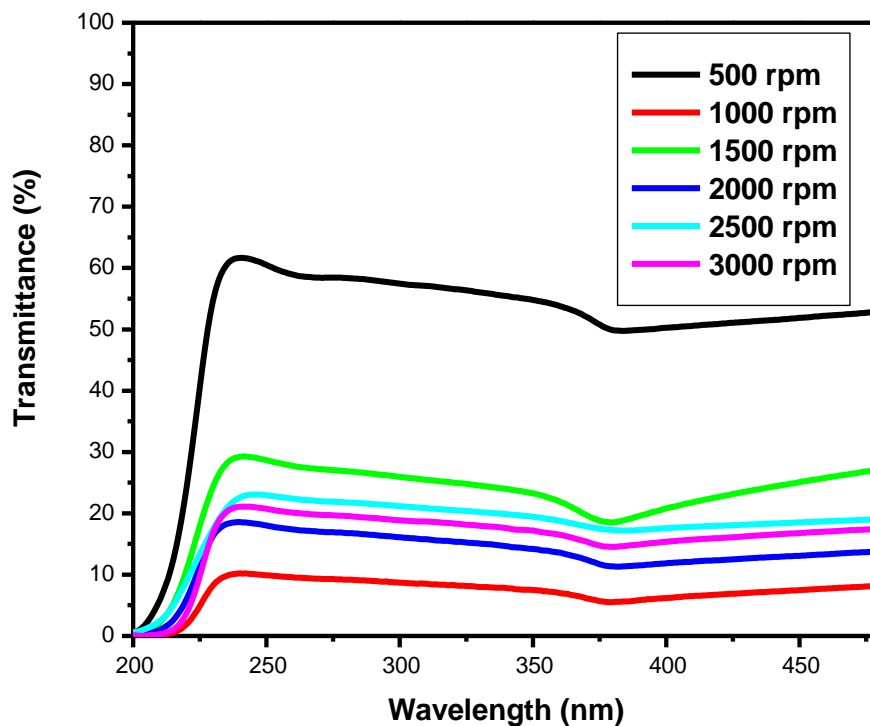


**Figure 2(i).** UV-Vis spectrum showing transmittance (%) against wavelength (nm) of as prepared ZnO:Al:Ga co-doped nanoparticles for varying stirring speed

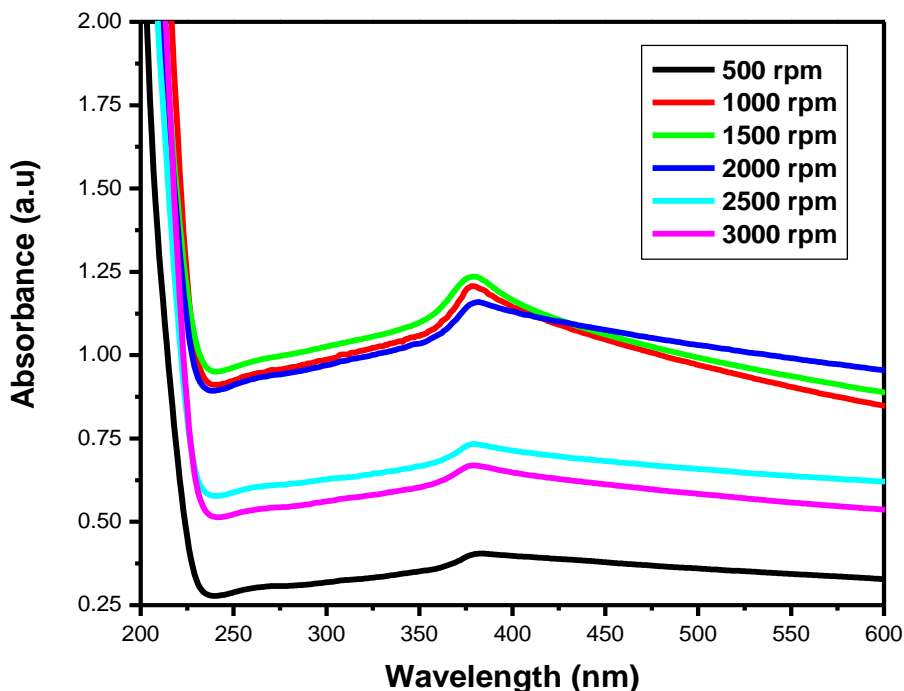


**Figure 2(ii).** UV-Vis spectrum absorbance (a.u) against wavelength (nm) of ZnO:Al:Ga co-doped nanoparticles with varying stirring speed

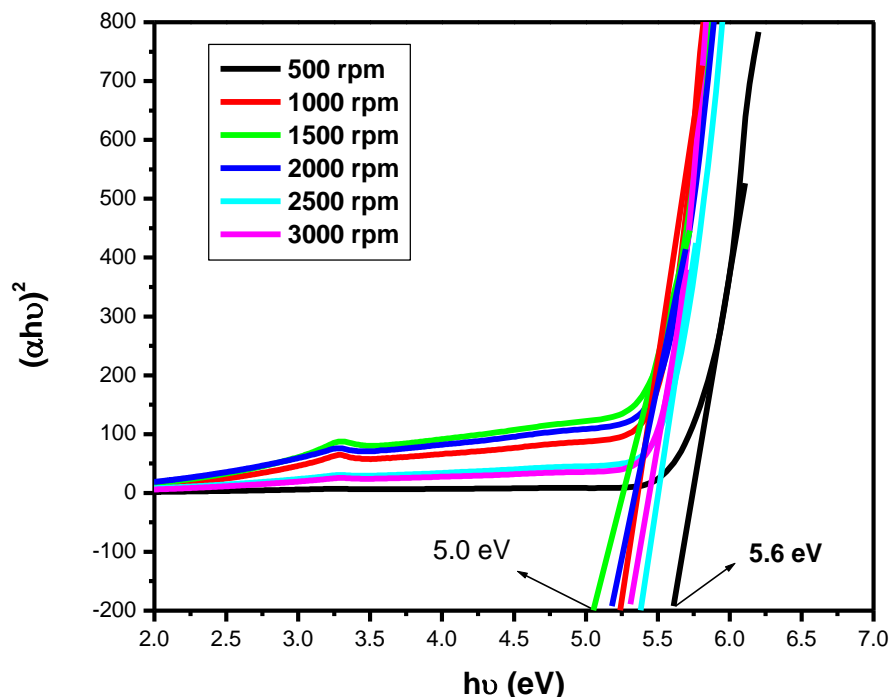


**Figure 2(iii).** Tauc's plot of ZnO:Al:Ga co-doped nanoparticles with varying stirring speed

Further supporting the sensitivity of optical properties to synthesis stirring speed is the fact that, as shown in Figure 2(ii), the absorbance spectra of ZnO:Al:Ga co-doped nanoparticles at wavelength range (377 - 379 nm) reflect the absorbance spectra seen by Rahman Khan et al. (2018). Complementing spectral analysis, by the equation  $E_g = \frac{hc}{\lambda}$  where  $h$  is the Plank's constant  $c$  is the velocity of light and  $\lambda$  is the absorbance peak. The ZnO:Al:Ga co-doped nanoparticles' resultant energy band gaps are listed in Table 4 for each stirring speed. The energy band-gaps findings, which are around 3.27 and 3.29 eV, support patterns seen in earlier studies by Droepenu et al. (2022), who also found that stirring speed had a significant impact on band gap energies in zinc oxide nanoparticles. The control of stirring speeds at optimum enhance good nanoparticles with light absorption and electron transport.

**Table 4.** Summarize table of wavelength and energy band gap

sample	Wavelength (nm)	$E_{bg}$ (eV)
500 rpm	379	3.27
1000 rpm	378	3.28
1500 rpm	377	3.29
2000 rpm	379	3.27
2500 rpm	379	3.27
3000 rpm	378	3.28

The optical properties of ZnO:Al:Ga co-doped nanoparticles under different stirring speeds was by analyzed Tauc's plot extrapolation in figure 2(iii). This is an established technique for estimating semiconductor's band-gap energy from its

absorbance spectrum. The estimated of the band-gaps energy were obtained by a graph of  $(\alpha h\nu)^2$  against the photon energy  $(h\nu)$  and using linear extrapolation to the x-axis. Band-gap energy values between 5.0 and 5.6 eV were found in this investigation at stirring rates between 500 and 3000 rpm. The band-gap energy change with stirring speed. Regarding the variance in the standard band-gap energy of 3.37 eV ZnO, the existence of defects or impurities in the nanoparticles as well as doping with Al and Ga could cause differences. According to Singh et al. (2019), doping can bring energy levels into the band-gap, changing the material's overall electronic structure. Furthermore, alterations in the synthesis circumstances and techniques can result in changes to the size, shape, and crystallinity of nanoparticles, all of which can affect the band-gap energy (Droepenu et al., 2022).

### SEM Analysis

SEM micrographs showing observable differences in particle size and shape throughout a range of stirring speeds are displayed in Figure 3(i). Similar findings were reported by Niroula (2022). For the ZnO:Al:Ga co-doped nanoparticles synthesized at 500 rpm, shows greater grain sizes, while those produced at 2500 rpm and 3000 rpm show smaller sizes with a porous texture. Higher stirring speeds facilitated more effective mixing and nucleation, resulting in to finer nanoparticles with more surface area and porosity indicating the improved nanoparticles since increase in the crystallite size improves the quality or properties of nanoparticles. These are favorable characteristics for improving charge transport and light absorption in solar cells, according to this phenomena.

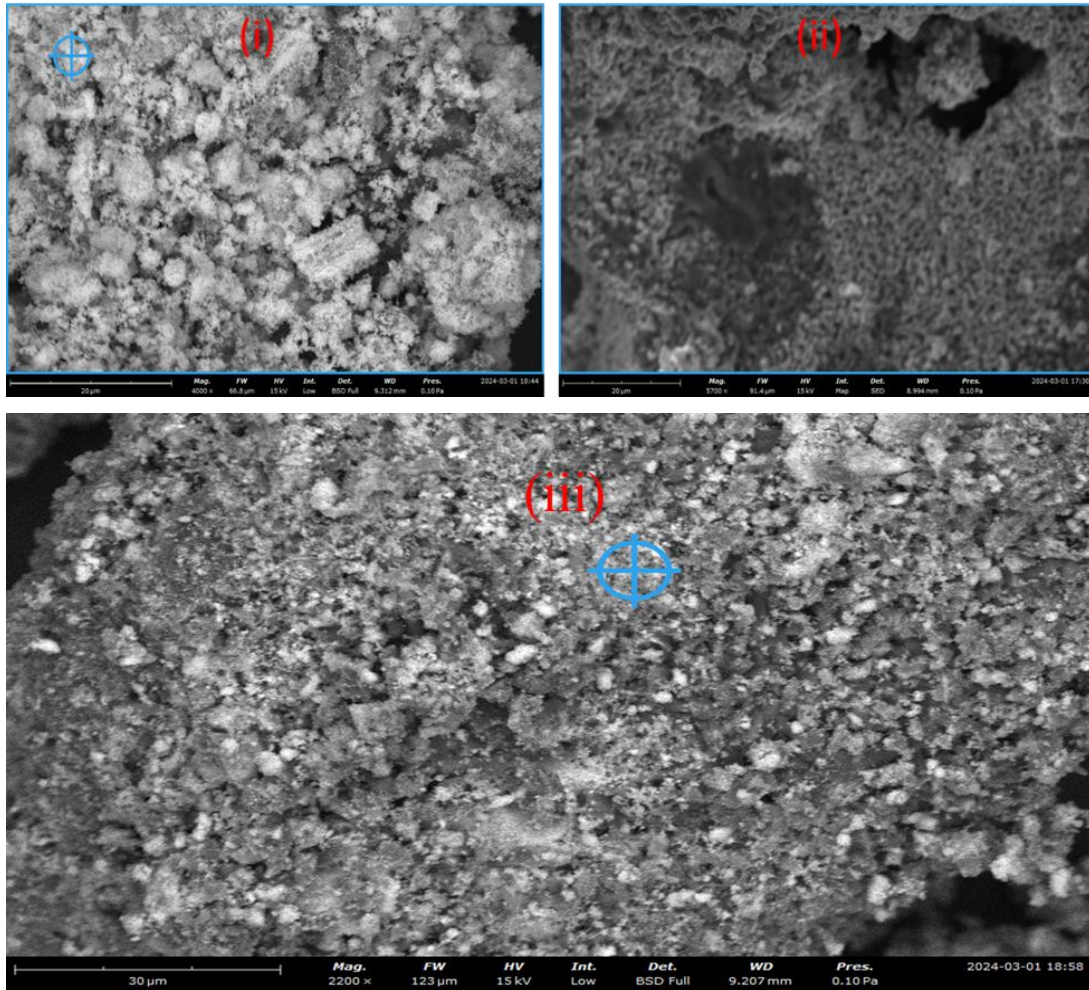


**Figure 3(i).** SEM micrographs of synthesized ZnO:Al:Ga co-doped nanoparticles under varying stirring speed (i) 500 rpm, (ii) 2500 rpm (iii) 3000 rpm

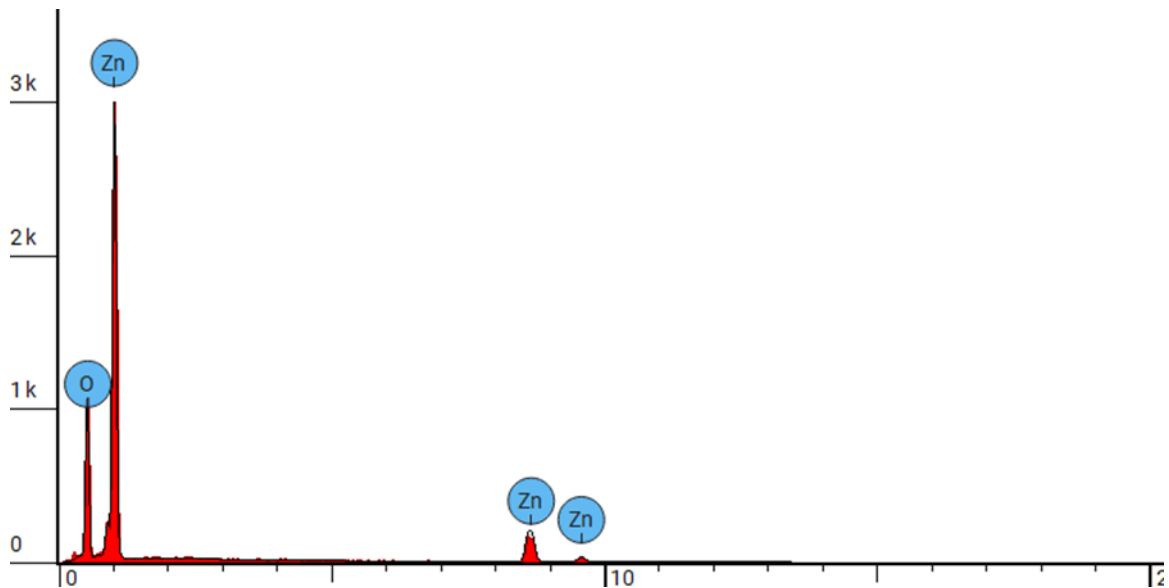


**Figure 3(ii).** Showing EDS elemental spectrum pattern synthesized ZnO:Al:Ga co-doped nanoparticles with stirring speed 500 rpm

Furthermore, Figure 3 (ii) – (iv) shows EDS elemental spectrum analysis, which confirms hexagonal wurtzite structure, clarifies the crystalline nature of the prepared nanoparticles. The crystalline nanostructure does not change even with

changes in stirring speed, indicating that particle size and shape are more affected by stirring condition changes than the crystalline phase (Sbeta, 2018). This result highlights the synthesis process's resilience and offers good information

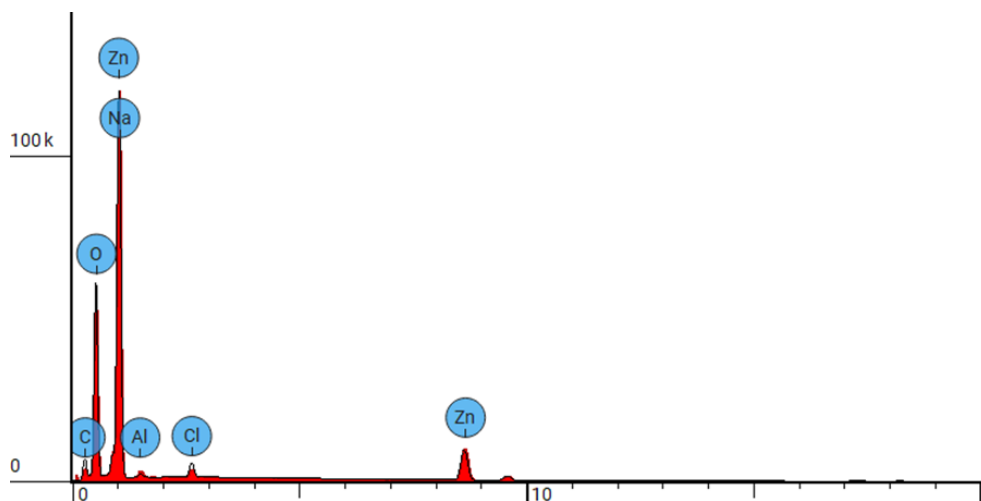
regarding the stirring speed and nanoparticle properties that are suitable to use in solar cells so as to produce high energy efficiency.

Moreover, all produced nanoparticles contain the necessary elements zinc and oxygen, according to elemental composition analysis in Tables 5, 6, and 7. At higher stirring speeds,

contaminants such as carbon, salt, aluminum, and chlorine are found. Impurity presence, especially at high stirring speeds, indicates possible contamination or unfinished synthesis processes, underscoring the significance of stirring condition optimization to reduce impurity incorporation and guarantee nanoparticle purity for intended applications.

**Table 5.** Showing elements of synthesized ZnO:Al:Ga co-doped nanoparticles with stirring speed 500 rpm

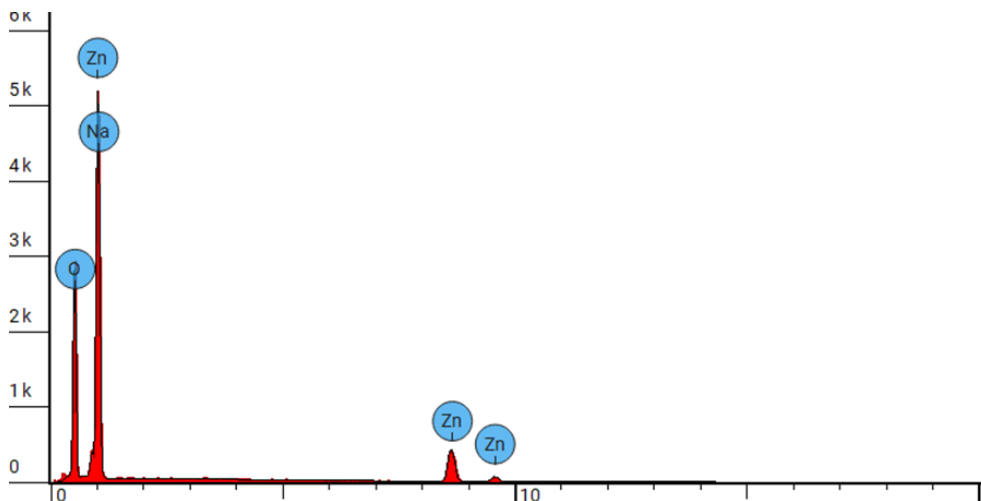
	Element Number	Element Symbol	Element Name	Atomic Conc.	Weight Conc.
	8	O	Oxygen	61.022	27.700
	30	Zn	Zinc	38.978	72.300



**Figure 3(iii).** Showing EDS elemental spectrum pattern synthesized ZnO:Al:Ga co-doped nanoparticles with stirring speed 2500 rpm

**Table 6.** Showing elements of synthesized ZnO:Al:Ga co-doped nanoparticles with stirring speed 2500 rpm

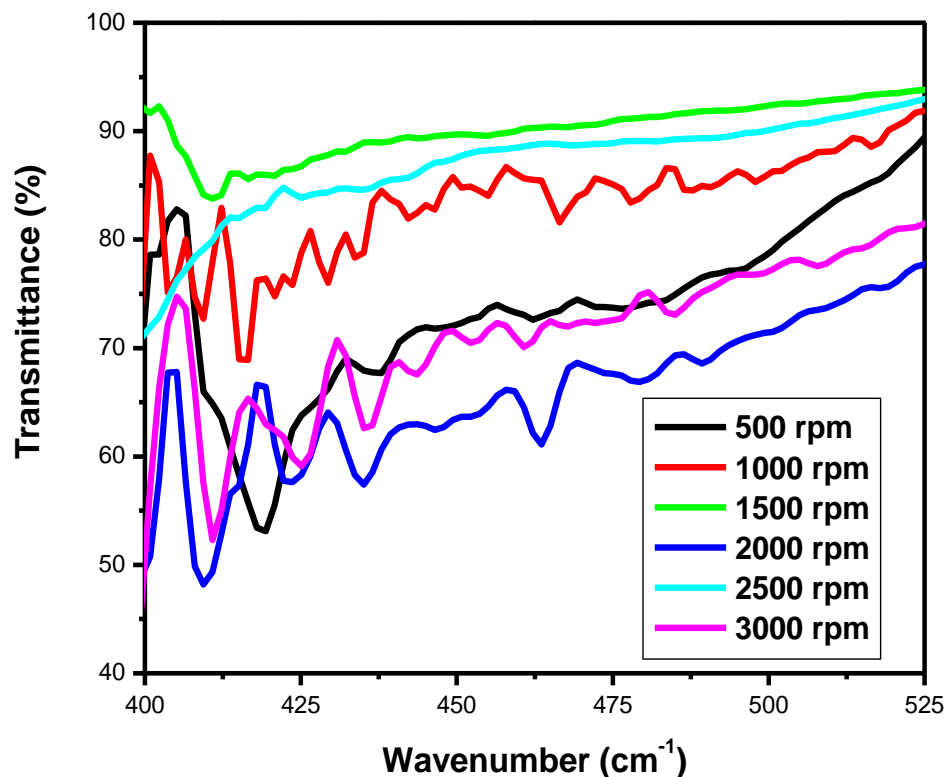
	Element Number	Element Symbol	Element Name	Atomic Conc.	Weight Conc.
	6	C	Carbon	21.394	11.211
	8	O	Oxygen	44.163	30.831
	11	Na	Sodium	20.448	20.521
	13	Al	Aluminum	0.425	0.501
	17	Cl	Chlorine	1.359	2.102
	30	Zn	Zinc	12.211	34.835



**Figure 3(iv).** Showing EDS elemental spectrum pattern synthesized ZnO:Al:Ga co-doped nanoparticles with stirring speed 3000 rpm

**Table 7.** Showing elements of synthesized ZnO:Al:Ga co-doped nanoparticles with stirring speed 3000 rpm

	Element Number	Element Symbol	Element Name	Atomic Conc.	Weight Conc.
	8	O	Oxygen	54.676	31.832
	11	Na	Sodium	25.716	21.522
	30	Zn	Zinc	19.608	46.647

**Figure 4.** FTIR spectrum % transmittance against wavenumber ( $\text{cm}^{-1}$ ) of ZnO:Al:Ga co-doped nanoparticles under varying stirring speed

### FTIR Analysis

FTIR analysis makes it possible to identify and characterize important chemical bonds, such as the bonding wavenumbers of Al-O, Zn-O, and Ga-O that are present in the nanoparticles. Figure 4 shows the FTIR spectra of synthesized nanoparticle. The transmittance against wavenumber between 400- 500  $\text{cm}^{-1}$  are the stretching vibration modes of zinc-oxygen (Zn-O) bonding. This is in a line with the research done by Aleksandrova et al. (2022), which reported aluminum-oxygen (Al-O) bonding is observed in the 600–800  $\text{cm}^{-1}$  region, gallium-oxygen (Ga-O) bonding seen in 500–800  $\text{cm}^{-1}$  region and similarly zinc-oxygen (Zn-O) bonding takes place in the region 400–500  $\text{cm}^{-1}$  range. These bonding wavenumbers provide important details regarding the nanoparticles' functional groups and chemical- bonding units. Different stirring speeds during synthesis affect the chemical-bonding structure of the nanoparticles, as indicated by variations in the intensity or position of these peaks in FTIR spectrum in figure 4. Additionally, knowing the properties of Al-O, Zn-O, and Ga-O chemical bonds' bonding helps in supporting the elemental analysis done by SEM verifying the synthesized nanoparticles. As well as the distinct spectrum of different stirring speeds chemical-

bonding within the prepared nanoparticles.

## 4. Conclusions

ZnO:Al:Ga co-doped nanoparticles synthesized and characterized for solar cell applications at different stirring speeds have revealed a plethora of information that is essential for the advancement of renewable energy technology. The identification of a hexagonal wurtzite phase by XRD analysis offers a strong basis for comprehending the structural properties of the nanoparticles. This affirms that sol-gel technique is successful method of synthesis with desirable qualities of nanoparticles. Also, the resulting crystallite size of 21.46 - 20.61 nm showed improved nanoparticles. The optical properties are clarified by UV-Vis spectroscopy, which is necessary for effective light absorption and transmittance. The absorbance spectra of ZnO:Al:Ga co-doped nanoparticles registered wavelength range 377 - 379 nm equivalent to the energy band-gaps 3.27 and 3.29 eV respectively. This corresponds to the standard ZnO's energy band-gap but contrary to the tauc's plot estimation. SEM imaging demonstrated uniform distribution within the nanoparticles but that shape varies with speed, with higher

speeds of 3500rpm producing smaller nanoparticles while lower speed of 500rpm showed large morphological particle grain-like sizes. EDS examination reveals stirring speed-induced contaminants and validates the existence of key elements. The lower speed showed less incorporation of imperfections while higher speeds showed contamination of nanoparticles. Surface functionalization and chemical composition was better understood with the use of FTIR analysis which confirmed M-O chemical-bonding as evidenced by vibrations modes between 400 – 500  $\text{cm}^{-1}$ . The findings of the study showed stirring speed of 1000 rpm as good stirring velocity of the precursor. The speed of 1000 rpm was accompanied with the minimal imperfections and impurities as shown by the values of dislocation density and strain. The highest crystallite size at 1000rpm also support. Furthermore the band-gap of wavelength 378 nm from the UV-vis absorbance spectrum with the FTIR showing more stretching vibrations modes with the region of 400 – 500  $\text{cm}^{-1}$ . All these finding supports 1000 rpm as the effective stirring speed for synthesizing nanoparticle for possible solar cells with improved device performance, both of which support the long-term growth of clean energy sources.

## ACKNOWLEDGEMENTS

This research has been successful through the financial support received from African AI Research grant Award: DSA and Deep Learning Indaba. The authors wish to thank this team and Murang'a University of Technology for giving us access to various synthesis and characterization techniques for the research.

## Declaration of Conflict of Interest

The authors have no conflict of interest to declare.

## REFERENCES

- [1] Afre, R. A., Sharma, N., Sharon, M., & Sharon, M. (2018). Transparent conducting oxide films for various applications: A review. *Reviews on advanced materials science*, 53(1), 79-89.
- [2] Aleksandrova, M., Dobrikov, G., Pathan, H., Sartale, S., & Videkov, V. (2022). Study of front panel electrode coatings for combined visible and short wavelength infrared photodetectors. *Materials Today: Proceedings*, 54, 57-62.
- [3] Chakraborti, D. (2008). Novel diluted magnetic semiconductor materials based on zinc oxide.
- [4] Droepenu, E. K., Wee, B. S., Chin, S. F., Kok, K. Y., & Maligan, M. F. (2022). Zinc oxide nanoparticles synthesis methods and its effect on morphology: A review. *Biointerface Res. Appl. Chem*, 12, 4261-4292.
- [5] Eswar, K. A., Rostan, N. F., Mohamad, M., Akhir, R. M., Azhar, N. A. K., Buniyamin, I., ... & Abdullah, S. (2024). The Structure of Epitaxial Growth of Nb-doped ZnONanorods on Intrinsic Substrate via Sonicated Aqueous Chemical Method. *Ceramics International*.
- [6] Gakuru Simon Waweru, Sharon Kiprotich, Peter Waithaka (2024). Effects of Different Zn Doping Concentration on the Optical and Structural Properties of  $\text{TiO}_2$  Nanoparticles, *Nanoscience and Nanotechnology*, 13(1), 1-9.
- [7] Gatou, M. A., Kontoliou, K., Volla, E., Karachalios, K., Raptopoulos, G., Paraskevopoulou, P., ...& Pavlatou, E. A. (2023). Optimization of ZnO nanoparticles' synthesis via precipitation method applying taguchi robust design. *Catalysts*, 13(10), 1367.
- [8] Geetha, V. (2020). *Fabrication of Zinc Oxide Based Nanostructures for Light Emission and Gas Sensing Applications* (Doctoral dissertation, Research department of physics Government victoria college, Palakkad, University of Calicut.).
- [9] Gherbi, B., Laouini, S. E., Meneceur, S., Bouafia, A., Hemmami, H., Tedjani, M. L., ... & Mena, F. (2022). Effect of pH value on the bandgap energy and particles size for biosynthesis of ZnO nanoparticles: Efficiency for photocatalytic adsorption of methyl orange. *Sustainability*, 14(18), 11300.
- [10] Kelchtermans, A. (2014). Synthesis and in-depth characterization of Al-doped ZnO nanoparticles as building blocks for TCO layers.
- [11] Khan, M. F., Ansari, A. H., Hameedullah, M., Ahmad, E., Husain, F. M., Zia, Q., ... & Aliev, G. (2016). Sol-gel synthesis of thorn-like ZnO nanoparticles endorsing mechanical stirring effect and their antimicrobial activities: Potential role as nano-antibiotics. *Scientific reports*, 6(1), 1-12.
- [12] Kiprotich, S., Dejene, F. B., & Onani, M. O. (2022). Effects of growth time on the material properties of CdTe/CdSe core/shell nanoparticles prepared by a facile wet chemical route. *Materials Research Express*, 9(2), 025008.
- [13] Lewis, N. S., & Nocera, D. G. (2006). Powering the planet: Chemical challenges in solar energy utilization. *Proceedings of the National Academy of Sciences*, 103(43), 15729-15735.
- [14] Liang, Z., Zhang, Q., Jiang, L., & Cao, G. (2015). ZnO cathode buffer layers for inverted polymer solar cells. *Energy & Environmental Science*, 8(12), 3442-3476.
- [15] Mukwakwa, N. (2017). *Deposition of zinc oxide thin films by spin coating and examination of their structural, electrical and optical characteristics for solar cell application* (Doctoral dissertation, The University of Zambia).
- [16] Nagorski, M. (2021). *Optimization of the process for sol-gel derived ZnO: Al thin films for transparent conducting oxide applications* (Doctoral dissertation).
- [17] Niroula, P. (2022). *Optimization of Nanocrystalline Metal Oxides-based Gas Sensors for Hydrogen Detection* (Doctoral dissertation, The University of Toledo).
- [18] OTHMANE, M. (2018). *Synthesis and characterization of Zinc Oxide (ZnO) Thin films deposited by spray pyrolysis for applying: electronics and photonics* (Doctoral dissertation, UNIVERSITE MOHAMED KHIDER BISKRA).
- [19] Rahman Khan, M. M., Akter, M., Amin, M. K., Younus, M., & Chakraborty, N. (2018). Synthesis, luminescence and thermal properties of PVA-ZnO-Al<sub>2</sub>O<sub>3</sub> composite films:

- towards fabrication of sunlight-induced catalyst for organic dye removal. *Journal of Polymers and the Environment*, 26, 3371-3381.
- [20] Sbeta, M. N. (2019). Integration of sol-gel derived doped zinc oxide films and solution-processed metal nanoparticles for thin film photodiode and solar cell applications.
- [21] Shaba, E. Y., Jacob, J. O., Tijani, J. O., & Suleiman, M. A. T. (2021). A critical review of synthesis parameters affecting the properties of zinc oxide nanoparticle and its application in wastewater treatment. *Applied Water Science*, 11(2), 48.
- [22] Singh, P., Kumar, R., & Singh, R. K. (2019). Progress on transition metal-doped ZnO nanoparticles and its application. *Industrial & Engineering Chemistry Research*, 58(37), 17130-17163.
- [23] Ungula, J., Kiprotich, S., Swart, H. C., & Dejene, B. F. (2022). Investigation on the material properties of ZnO nanorods deposited on Ga-doped ZnO seeded glass substrate: Effects of CBD precursor concentration. *Surface and Interface Analysis*, 54(10), 1023-1031.
- [24] Ungula, J., Kiprotich, S., & Swart, H. C. (2024). Effect of Deposition Time on Material Properties of ZnO Nanorods Grown on GZO Seed Layer by CBD. *Journal of Nanosciences Research & Reports. SRC/JNSRR-170*. DOI: doi. org/10. 47363/JNSRR/2024 (6), 156, 2-6.
- [25] Zak, A. K., Esmailzadeh, J., & Hashim, A. M. (2024). X-ray peak broadening and strain-driven preferred orientations of pure and Al-doped ZnO nanoparticles prepared by a green gelatin-based sol-gel method. *Journal of Molecular Structure*, 1303, 137537.
- [26] Zhou, Y., Chen, J., Bakr, O. M., & Sun, H. T. (2018). Metal-doped lead halide perovskites: synthesis, properties, and optoelectronic applications. *Chemistry of Materials*, 30(19), 6589-6613.